Confinement of a hydrophilic polymer in membrane lyotropic phases

R. López-Esparza [a,*], M.A. Guedeau-Boudeville [b], E. Larios-Rodríguez [c], A. Maldonado [a], R. Ober [d], W. Urbach [e]

[a] *Departamento de Física, Universidad de Sonora, Apdo. Postal 1626, 83000 Hermosillo, Sonora, Mexico*
[b] *Laboratoire Matière et Systèmes Complexes (MSC), UMR 7057, CNRS, Université Paris-Diderot, Paris, France*
[c] *Posgrado en Materiales, Universidad de Sonora, 83000 Hermosillo, Sonora, Mexico*
[d] *Laboratoire de Physique de la Matière Condensée, Collège de France, Paris, France*
[e] *Laboratoire de Physique Statistique, Ecole Normale Supérieure, 24 rue Lhomond, Paris, France*

ABSTRACT

We study the confinement of a hydrophilic polymer (polyethylene glycol or PEG) between the bilayers of the zwitterionic surfactant tetradecyldimethyl aminoxide (C_{14}DMAO). Small angle X-ray scattering and electron microscopy experiments show that the polymer modifies the physical properties of the lyotropic smectic (L_α) phase. The observed effects are similar to those reported for anchored hydrophobically-modified polymers, indicating a strong interaction between PEG and the C_{14}DMAO bilayers. Self-diffusion experiments performed in the lyotropic sponge (L_3) phase show that the polymer adsorbs onto the surfactant membranes. This adsorption explains earlier observations: high polymer concentrations decrease the Gaussian rigidity of the membranes and a vesicular phase is stabilized.

© 2008 Elsevier Inc. All rights reserved.

1. Introduction

In recent years there has been a growing interest in the physics of aqueous systems composed of mixtures of surfactants and polymers [1,2]. In some applications, it is desirable to have at the same time properties given by the surfactant (detergency, wettability, foaming, emulsification, etc.) as well as properties provided by the polymer (viscosity, protective layers, etc.). Sometimes, the mixed systems have characteristics differing from those of the pure components due to the formation of a polymer–surfactant complex. This is easy to understand when an ionic surfactant interacts with a polymer of different electric charge. However, some non-ionic surfactants also form complexes with neutral polymers probably due to hydrogen bonding between the polymer and the surfactant polar head [3–5]. The few experiments reported in the literature with these neutral systems have been performed in the micellar surfactant phase.

But the phases composed of surfactant bilayers are also of interest for its implications in soft-condensed matter and in biology. Although their importance, no systematic experiments have been reported on non-ionic surfactant bilayers—neutral polymer mixed systems. Surfactant bilayers are self-assembled two-dimensional fluid structures [6]. The simplest bilayer phase is the lamellar phase, L_α, a smectic A lyotropic liquid crystal. It is composed of a periodic stack of surfactant bilayers separated by a solvent. On the other hand, sponge or L_3 phases are formed by a continuous, randomly-connected isotropic network of surfactant bilayers. Both phases are present in neighboring regions in several phase diagrams and their structure have been well characterized by techniques such as small-angle X-ray scattering (SAXS) and freeze-fracture electron microscopy (FFEM).

Recently, the effect of adding the water-soluble neutral polymer polyethylene glycol (PEG) to the lamellar phase of a zwitterionic surfactant system has been studied [7]. SAXS and FFEM experiments revealed that the polymer induces the spontaneous formation of highly monodisperse multilayered vesicles. These structures appear when the polymer concentration reaches a value of the order of 5 g/l, while keeping constant the membrane volume fraction [6]. Below this PEG concentration, the macroscopic features of the lamellar phases (transparency, birefringence) are very similar. In order to explain this surprising effect, it has been assumed that the polymer adsorbs onto the surfactant bilayers, triggering a topology transition from flat, open bilayers (lamellar phase) to closed aggregates (vesicles).

In this paper we report experiments on the effect of PEG on the lamellar and sponge phases of the same zwitterionic surfactant system reported in Ref. [7]. However, in the present work the polymer concentration is kept below the value which produces the multilayered vesicles. In this way, we study these phases prior to phase transformation. We have performed FFEM and SAXS experiments in lamellar and sponge phases with increasing polymer concentration. We have also performed fluorescence recovery after
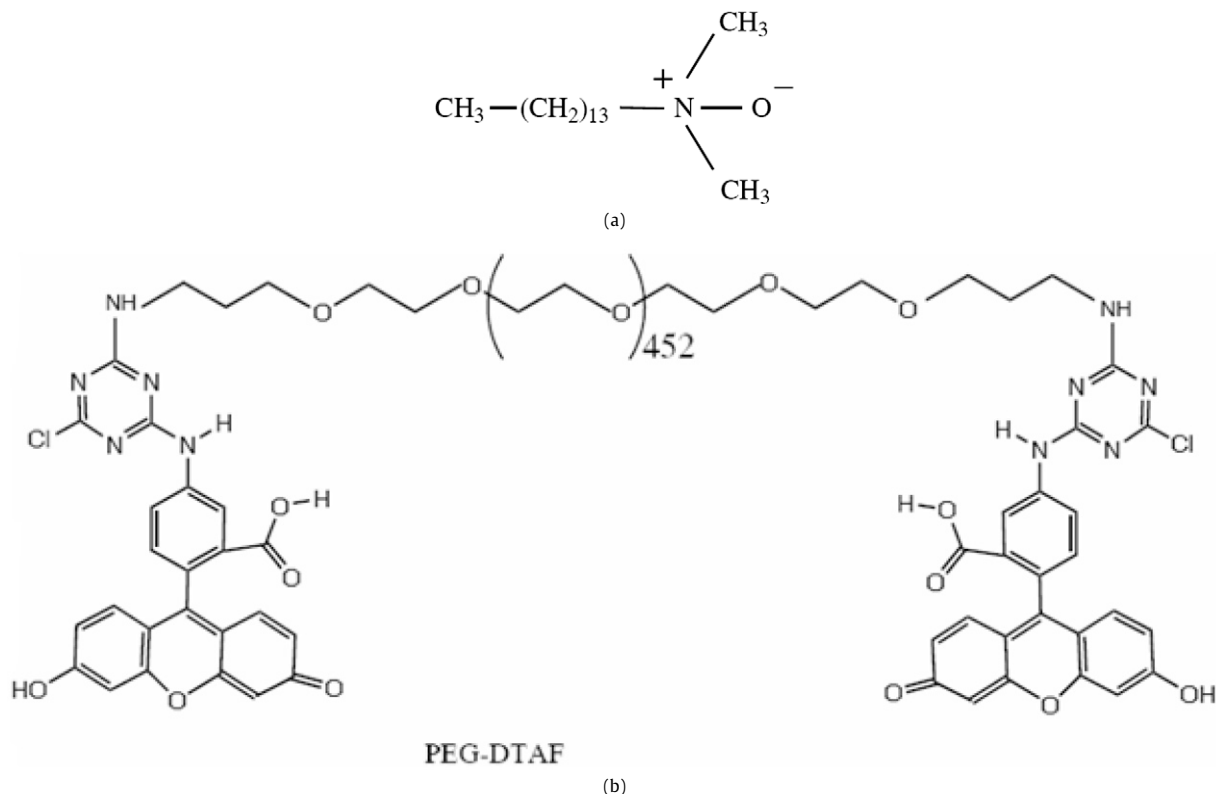
Fig. 1. Chemical structure of the molecules used in this work: (a) surfactant (C_{14}DMAO) and (b) fluorescent PEG (PEG-DTAF). This polymer has been used in the FRAPP experiments. For the other experiments, we used the same polymer (PEG) without the fluorescent groups shown at both ends of the molecule.

pattern photobleaching (FRAPP) experiments in order to measure the self-diffusion coefficient of PEG in sponge phases. For this, the polymer has been modified with a fluorescent dye. Neither the use of fluorescent PEG nor FRAPP experiments was reported in Ref. [7]. Our aim is to obtain some insight into the influence of the polymer on the physical properties of the lamellar and sponge phases, and to determine whether or not the polymer adsorbs onto the surfactant bilayers.

The paper is divided as follows. In Section 2 we describe the experimental techniques used and the methods for preparing the samples. In Section 3 we present and discuss our experimental results and in Section 4 we draw some conclusions.

2. Experimental

2.1. Materials

Tetradecyldimethyl aminoxide (C_{14}DMAO) which was recrystallized twice, was a gift from Dr. H. Hoffmann. It is a zwitterionic surfactant that behaves like a non-ionic in neutral or alkaline solutions as in our case [8]. Fluorescein-5-isothiocyanate (FITC 'Isomer I') was purchased from Molecular Probes. Poly(ethylene glycol) (PEG) of molecular weight 20,000 g/mol and 5-(4,6-dichloro-s-triazin-2-ylamino) fluorescein hydrochloride ($C_{23}H_{12}Cl_2N_4O_5$HCl or DTAF) were purchased from Sigma and used as received. In order to follow the polymer diffusion with the FRAPP technique, we labeled PEG molecules with a fluorescent dye, according to the DTAF labeling of dextran [9]. Materials, synthesis details, and purification steps are described in detail in a previous article [10]. All samples were prepared in ultra-purified water (resistivity ≈ 18 MΩ cm). In Fig. 1 we show the chemical structure of the surfactant (C_{14}DMAO) as well as the polymer (fluorescent-PEG) we used.

2.2. Samples and experimental methods

The lamellar (L_α) and sponge (L_3) phases are prepared in the ternary system formed by the zwitterionic surfactant (tetradecyldimethyl aminoxide or C_{14}DMAO), hexanol (cosurfactant) and water as solvent. The phase diagram displays a large range of bilayer volume fractions, ϕ, where both the L_α and L_3 phases are stable; this range is roughly $0.05 \leqslant \emptyset \leqslant 0.3$ [10]. For a given bilayer volume fraction, the difference between the lamellar and sponge regions is the cosurfactant to surfactant mass ratio $r = \frac{m_{hex}}{m_{C_{14}DMAO}}$. For the studied bilayer volume fractions, we have prepared lamellar phases with $r \approx 0.85$ and sponge phases with $r \approx 0.89$. For preparing each sample, the appropriate amount of C_{14}DMAO was weighted in a test tube. Ultrapure water was added and the surfactant was allowed to dissolve completely. Finally, hexanol was added drop by drop while mixing until the desired $\frac{m_{hex}}{m_{C_{14}DMAO}}$ ratio was reached. The lamellar phase was assessed by observing the typical birefringence between crossed polarizers. The sponge phase was assessed by detecting a drastic decay in viscosity at the same time as the phase appeared isotropic between crossed polarizers. The characteristic distance of the lamellar and sponge phases, d, depends on the bilayer volume fraction ϕ. PEG has been added to the lamellar and sponge phases in a concentration range between 0 and 8.5×10^{-5} M. These concentrations are below the limit that produces multilayered vesicles in the same system [7].

The structure of the lyotropic phases has been studied by SAXS in a Rigaku rotating anode set-up described elsewhere [11]. Samples for the FFEM experiments have been prepared in a Jeol Freeze Etching Equipment (JFD 9010). TEM observations have been made in a Jeol JEM 2010F apparatus. The self-diffusion coefficient was measured by the fluorescence recovery after pattern photobleaching (FRAPP) technique as described in a previous paper [12]. In order to follow the polymer diffusion with the FRAPP technique,
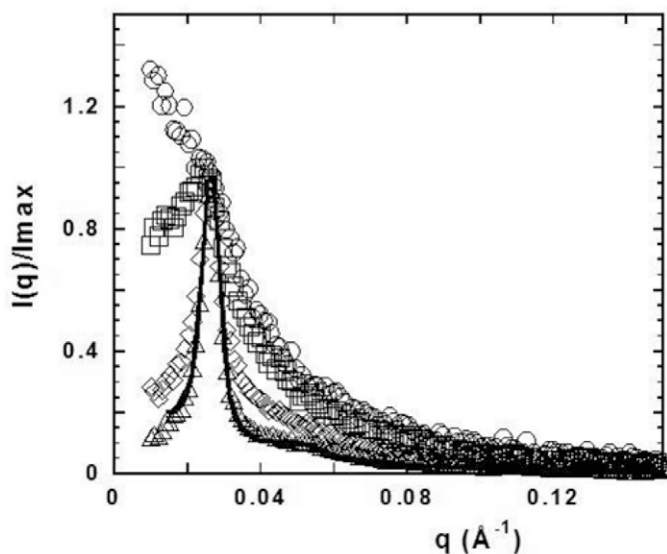
Fig. 2. Scattering spectra of lamellar phases with different polymer concentrations. The surfactant volume fraction in all samples is $\phi = 0.1$. Polymer concentrations are: 0 M (circles), 1.6×10^{-6} M (squares), 1.6×10^{-5} M (diamonds) and 8.4×10^{-5} (triangles). The solid line is a theoretical fit (see text).

we labeled PEG molecules with a fluorescent dye, according to the DTAF labeling of dextran [9]. In order to assess if the labeling procedure modifies the hydrodynamic radius of the polymer, we measured the diffusion coefficient of PEG in diluted water solutions, before and after labeling. For pure PEG we used Dynamic Light Scattering (DLS), while for fluorescent PEG we used FRAPP. The DLS experiments were performed in the homodyne mode using a 633 nm He–Ne laser and an ITI FW130 photomultiplier as light detector. The signal was digitized by an ALV-PM-PD amplifier-discriminator. The signal analyzer was an ALV-5000 digital multiple-r correlator. The intensity autocorrelation function was measured at 50°, 70°, 90°, and 110°. A similar experimental set-up has been used to study the effect of hydration on the hydrodynamic radius of PEG [13]. In our case, all the measured correlation functions were single exponentials. From them, the mutual diffusion coefficient was obtained. The diffusion coefficients obtained with the DLS and the FRAPP techniques agree within experimental error [10]. This means that the hydrodynamic radius of PEG is not appreciably modified by adding the fluorescent group.

3. Results and discussion

3.1. SAXS experiments: Lamellar phases

The scattering spectra of lamellar phases with different polymer concentrations C_{pol} are shown in Fig. 2. The bilayer volume fraction in these samples is $\phi = 0.1$. The data are shown after renormalizing the intensities $I(q)$ by their respective value at the peak position $I(q_{max})$. The polymer-free lamellar phase does not display the characteristic Bragg peak due to thermal fluctuations, which contribute to a high scattering in the low-q region that hides the expected peak. However, when polymer is added to the lamellar phase, the spectra display a well defined Bragg peak whose position does not show any shift when the polymer concentration is increased. Note that the value of q_{max} is the value expected at this volume fraction from the classical swelling law $q_{max} = \frac{2\pi\phi}{\delta}$, where the bilayer thickness is $\delta = 24$ Å [11]. Using the Bragg relation $q_{max} = 2\pi/d$, the interbilayer distance in the lamellar phases is $d = 240 \pm 2$ Å.

On the other hand, the polymer concentration does have an effect on the peak width and on the small-angle scattering sig-

nal. As one can see from the graphs, the peak clearly stiffens and the small-angle scattering becomes weaker with increasing C_{pol}. The same qualitative features are observed in SAXS spectra of the lamellar phases with higher bilayer volume fractions. Even if these effects are not completely monotonic (some samples, not shown in Fig. 2, deviate, probably due to small variations in cosurfactant concentration) they indicate that the polymer modifies the elastic properties of the bilayers. This is confirmed by the emergence of the Bragg peak when polymer is added to the lamellar phase. Note that the observed effects are similar to those produced by a hydrophilic polymer hydrophobically modified in order to anchor into neutral lamellar phases [14]. Our results seem to indicate that PEG binds to the C_{14}DMAO surfactant bilayers.

From the SAXS spectra one can get information on the elastic constants of the lamellar phase. The decrease in the width of the Bragg peak can be interpreted in terms of the Landau–Peierls exponent η that describes the power-law Caillé singularity $I(q) \approx |q - q_{max}|^{-1+\eta}$. In this equation, η is the Caillé parameter, related to the peak position q_{max} and the interbilayer distance in the lamellar phase, d:

$$\eta = \frac{q_{max}}{8\pi\sqrt{\frac{k\bar{B}}{d}}}. \tag{1}$$

In this equation, k is the bending elastic constant of the bilayer, defined in the Helfrich curvature free energy of the membrane [15]; $\bar{B}$ is the compression modulus of the smectic phase. We extracted η values from the scattering spectra by fitting the data to a well-established theory combining geometry of the bilayers and membrane-displacement fluctuations [16]. The fits were rather poor for low polymer concentrations but improve considerably for the highest C_{pol} (Fig. 2). From the fit, we found $\eta = 0.39$ for the highest C_{pol}. The qualitative effect of an increasing polymer concentration is to decrease the value of the parameter η. From Eq. (1), this means that the product kB increases as polymer is added to the lamellar phase. We have no way to estimate the contribution of k to the decrease of η. However, it is well known that the observed decrease in the intensity at low angles (Fig. 2) corresponds to an increase of $\bar{B}$. That is, the smectic phase compression modulus increases with polymer concentration. A larger smectic modulus $\bar{B}$ indicates a stiffening of the intermembrane interaction potential.

Note that for polymer concentrations $C_{pol} > 2.5 \times 10^{-4}$ M the SAXS spectra are modified (not shown in Fig. 2). The small-angle scattering increases and the peak position shifts to smaller interbilayer distances. These effects are due to the apparition of closed aggregates (vesicles) as shown in the electron microscopy picture (Fig. 3). These big aggregates scatter in the low-q region and may contribute to the small-angle scattering signal. A detailed description of the experiments with the vesicle phases is given in Ref. [7], where the studied PEG concentrations were higher than those reported in the present paper.

3.2. SAXS experiments: Sponge phases

Before performing the FRAPP experiments with the sponge phase, we studied with SAXS its structure with increasing polymer concentrations. In Fig. 4 we show the scattering spectra for sponge phases with different PEG concentrations but fixed bilayer volume fraction ($\phi = 0.2$). The used PEG concentrations are: 2.1×10^{-6} M (circles), 8.4×10^{-6} M (squares) and 3.4×10^{-5} M (diamonds) and 8.4×10^{-5} M (triangles). As we can observe, the scattering spectra superpose within experimental error in a single curve. In addition, the macroscopic properties of the sponge phase (transparency, isotropy, single-phase) are not modified after addition of the polymer at these concentrations, as revealed by a visual inspection of

Fig. 3. FFEM picture of a closed aggregate (vesicle) observed in a lamellar phase with intermediate polymer concentration.
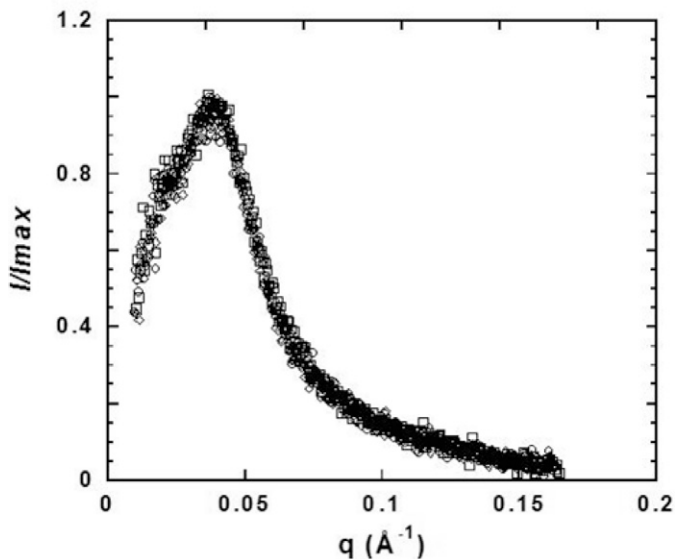

Fig. 4. Scattering spectra for sponge phases with PEG concentrations: 2.1×10^{-6} M (circles), 8.4×10^{-6} M (squares) and 3.4×10^{-5} M (diamonds). In all samples, the surfactant volume fraction is $\phi = 0.2$.

the samples. The same behavior (SAXS and visual inspection) has been observed for the other bilayer volume fractions. This means that, at least for these polymer concentrations, the sponge phase structure is the same. We can be sure that if any variation is found in the diffusion behavior of the polymer, it is due to a surfactant concentration effect and not to a phase transformation. In fact, for the FRAPP experiments, we worked within the polymer concentrations of Fig. 4 because the probe concentration has to be large enough to yield a good fluorescence recovery signal and small enough to avoid a strong absorption of light which can produce signal distortion and also heat convection in the samples. The optimal fluorescent PEG concentration for this is around 10^{-5} M. At such small concentrations, the sponge phases are not distorted by the polymer.

3.3. FRAPP experiments

In Fig. 5 we present the self-diffusion coefficient of the fluorescent polymer, as a function of surfactant volume fraction. In the dilute regime, the self-diffusion coefficient is nearly constant in
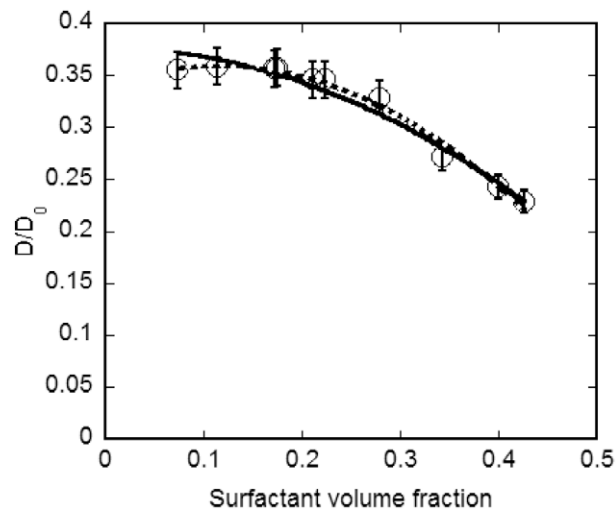

Fig. 5. Self-diffusion coefficient of the fluorescent polymer, as a function of surfactant volume fraction. The full line is a fit to the equation predicted by the diffusion equation for probes diffusing along the membranes of sponge phases (Eq. (3)). The broken line is a fit to the equation predicted when there is a partition between bound and unbound polymer molecules (Eq. (5)).

agreement with previous results obtained with other fluorescent probes [17]. For more concentrated samples, the self-diffusion coefficient decreases as the surfactant concentration increases.

We have interpreted these results in terms of the predictions reported in Ref. [18], where the diffusion equation was numerically solved for diffusing particles in sponge and cubic phases. It has been found that the dependence of the diffusion coefficient is different depending on where the Brownian motion occurs. For particles diffusing in the solvent of the phases, the diffusion coefficient D_{vol} decreases linearly with bilayer volume fraction

$$D_{vol}/D_{vol0} = a_{vol} - b_{vol}\phi. \tag{2}$$

In these equation, a_{vol} has a value around 2/3 and b_{vol} depends on the topology of the phase [18]. D_{vol0} is the self-diffusion coefficient of PEG in the solvent. We measured it with the FRAPP technique: $D_{vol0} = 7.4 \times 10^{-7}$ cm^2/s.

On the other hand, when the particles diffuse along the bilayers, the diffusion coefficient D_{bil} is:

$$D_{bil}/D_{bil0} = a_{bil} - b_{bil}\phi^2. \tag{3}$$

It has been shown analytically that $a_{bil} = 2/3$ [18]. The parameter b_{bil} also depends on the topology of the surface and has to be computed for every particular case [18]. D_{bil0} is the self-diffusion coefficient of the polymer on a flat membrane. Its measurement requires the orientation of the lamellar phase. However, we did not succeed in orientating a polymer-doped lamellar phase, so we could not measure D_{bil0}. Instead, we assumed a value of $D_{bil0} = 3.7 \times 10^{-7}$ cm^2/s, in order to get the analytic limit $D_{\phi \to 0} = (2/3)D_{bil0}$ in Eq. (3) [18]. Note however that the used D_{bil0} qualitatively agrees with the expected value because it has an order of magnitude between D_{vol0} and the self-diffusion coefficient of membrane proteins ($D_{protein} \sim 5 \times 10^{-8}$) [19]. Note that Eq. (3) should describe the diffusion of amphiphile molecules as well of molecules bound to the bilayers.

In Fig. 5, we can easily appreciate that the variation of D does not follow the linear decay (Eq. (2)) predicted for diffusing particles in the solvent of sponge phases. This is an indication that diffusion is not occurring completely in the volume between the surfactant bilayers. Another result pointing in this direction is the fact that the diffusion coefficient in the more diluted sponge phases has a relatively small value: $D_{\phi \to 0} = 0.35 D_{vol0}$, where

D_{vol0} is the diffusion coefficient of the polymer in a water solution ($D_{vol0} = 7.4 \times 10^{-7}$ cm^2/s). If diffusion were taking place in the space between the bilayers, the measured value should be $D_{\phi \to 0} \approx 0.6 D_{vol0}$ [18]. This result has been verified with two proteins as well as with a non-adsorbing water-soluble probe [17].

In order to assess if the polymer is diffusing along the bilayers of the sponge phase, in Fig. 5 we plot a fit to the quadratic decay predicted for this case (Eq. (3)). The agreement with theory is reasonably good within experimental error. This result suggests that for some fraction of PEG molecules diffusion takes place along the membranes, i.e., that the polymer binds to the surfactant and moves in the bilayer surface.

Note that in the preceding paragraphs we have assumed that all the polymer molecules either adsorb onto the surfactant bilayers or do not adsorb at all. However, it is possible to have some partition between adsorbed and non-adsorbed molecules. This point is particularly relevant since, even if PEG has a tendency to bind to interfaces [20], it is first of all a water-soluble polymer. So, in a more general situation, the observed diffusion coefficient, D_{obs}, is a weighted average of the bulk diffusion coefficient, D_{vol}, and the diffusion coefficient along the bilayers, D_{bil}. In this case, the observed diffusion coefficient can be written as

$$D_{obs} = (1-p)D_{bil} + pD_{vol}, \tag{4}$$

where p is the fraction of polymer molecules not adsorbed onto the surfactant bilayers, i.e., the fraction of molecules diffusing freely in the solvent. Of course, $0 < p < 1$. As we do not have a direct measurement of p, we can try to estimate it from a fit to the expressions describing D_{vol} and D_{bil}, as a function of surfactant volume fraction ϕ (Eqs. (2) and (3)) [18]. Using those equations, the observed diffusion coefficient can be more generally written as

$$D_{obs} = A - B\phi - C\phi^2, \tag{5}$$

where the constants are:

$$A = pa_{vol}D_{vol0} + (1-p)a_{bil}D_{bil0},$$

$$B = pb_{vol}D_{vol0},$$

and

$$C = (1-p)b_{bil}D_{bil0}.$$

In order to use these expressions, for D_{vol} and D_{bil} we take the values discussed in the previous paragraphs (7.4×10^{-7} cm^2/s and 3.7×10^{-7} cm^2/s, respectively). The constants b_{vol} and b_{bil} are topology-dependent. It is far from the scope of this paper to compute these values for each possibly topology. Instead, as an illustration we took the values obtained in Ref. [18] for the P family of minimal surfaces, a suitable model for sponge phases. These values are: $b_{vol} = 0.39$ and $b_{bil} = 0.45$. In addition, $a_{vol} = 0.65$ and $a_{bil} = 0.66$ [18].

With these considerations, we have fitted our experimental results to Eq. (5). The results are also shown in Fig. 5, where the fit to Eq. (5) is the broken line. The adjustment improves due to the linear term, probably meaning that a fraction of the polymer is actually diffusing in the solvent and other along the bilayers. However, due to the experimental slope of the data at low ϕ, we obtain a value of p with no physical meaning ($p > 1$). We conclude that more experiments should be performed in order to assess the fraction of PEG bound to the bilayers.

The FRAPP results described so far indicate that, to some extent, the polymer binds to the surfactant membrane. This result agrees with the interpretation of the SAXS spectra of the lamellar phases (Fig. 2). Both independent experiments points toward polymer adsorption onto the surfactant bilayers. In addition, the FRAPP results are qualitatively similar to those found with four amphiphilic probes diffusing in the membranes of the same system [12].

The binding of the polymer to the surfactant bilayers has an important consequence for their topology. In fact, adsorbing and non-adsorbing polymers have opposite contributions to the Gaussian term in the Helfrich elastic Hamiltonian, $E_G = \tilde{k}\frac{1}{R_1 R_2}$, $\tilde{k}$ is the bilayer Gaussian rigidity, and R_1 and R_2 are the principal radii of curvature of the membrane at any point. The Gaussian rigidity controls the topology of the membranes. When $\tilde{k}$ is positive, E_G is minimized when R_1 and R_2 have opposite signs, and saddle-like topologies are stabilized (sponge phases). On the other hand, when $\tilde{k}$ is negative, minimization of E_G requires R_1 and R_2 having the same sign; closed aggregates (vesicles) are stable. Theoretical results available for polymers adsorbing onto bilayers predict a decrease in $\tilde{k}$ [21].

This explains why larger concentrations of PEG added to a lamellar phase induce the formation of multilayered vesicles, as reported previously [7]: the adsorbing polymer decreases the Gaussian rigidity and thus stabilizes a lyotropic phase of closed aggregates (vesicles).

4. Conclusions

We have performed experiments on the effect of a neutral, water-soluble polymer, PEG, on the lamellar and sponge phases of a zwitterionic surfactant system: C$_{14}$DMAO–hexanol–water. The aim was to determine if binding of the polymer to the surfactant membranes occurs, as expected from a theoretical analysis of the polymer-induced lamellar-vesicular transformation reported previously for this system [7]. Both, SAXS and FRAPP experiments suggest that a fraction of the polymer molecules actually binds onto the surfactant bilayers. Although the fraction of bound polymer molecules could not be estimated by fitting our experimental data to an available theory [18], the binding of the polymer explains why larger concentrations of PEG added to the lamellar phase induce the formation of multilayered vesicles [7]. In fact, the polymer modifies the Gaussian rigidity of the membranes, thus triggering the phase transformation. Our FRAPP experiments show that by appropriately fluorescent-labeling polymer molecules, self-diffusion measurements can give some insight into polymer–surfactant interactions. More, specific experiments should be performed in order to determine the fraction of polymer molecules bound to the surfactant bilayers in this system.

References

[1] E.D. Goddard, K.P. Ananthapadmanabhan, Interaction of Surfactants with Polymers and Proteins, CRC Press, Boca Raton, FL, 1993.
[2] K. Holmberg, B. Jönsson, B. Kronberg, B. Lindman, Surfactants and Polymers in Aqueous Solution, Wiley, 2003.
[3] E. Feitosa, W. Brown, P. Hansson, Macromolecules 29 (1996) 2169.
[4] E. Feitosa, W. Brown, K. Wang, P.C.A. Barreleiro, Macromolecules 35 (2002) 201.
[5] K. Schillén, J. Jansson, D. Löf, T. Costa, J. Phys. Chem. B 112 (2008) 5551.
[6] W.M. Gelbart, A. Ben-Shaul, D. Roux (Eds.), Micelles, Membranes, Microemulsions, and Monolayers, Springer-Verlag, 1994.
[7] A. Maldonado, R. López-Esparza, R. Ober, T. Gulik-Krzywicki, W. Urbach, C.E. Williams, J. Colloid Interface Sci. 296 (2006) 365.
[8] C.A. Miller, M. Gradzielski, H. Hoffmann, U. Krämer, C. Thunig, Colloid Polym. Sci. 268 (1990) 1066.
[9] S. Prigent-Richard, M. Cansell, J. Vassy, A. Viron, E. Puvion, J. Jozefonvicz, D. Letourneur, J. Biomed. Mater. Res. 40 (2) (1998) 275.

[10] R. Lopez-Esparza, M.-A. Guedeau-Boudeville, Y. Gambin, C. Rodríguez-Beas, A. Maldonado, W. Urbach, J. Colloid Interface Sci. 300 (2006) 105.
[11] A. Maldonado, W. Urbach, R. Ober, D. Langevin, Phys. Rev. E 54 (2) (1996) 1774.
[12] A. Maldonado, W. Urbach, D. Langevin, J. Phys. Chem. B 101 (1997) 8069.
[13] C. Branca, S. Magazù, G. Maisano, F. Migliardo, P. Migliardo, G. Romeo, J. Phys. Chem. B 106 (2002) 10272.
[14] Y. Yang, R. Prudhomme, K.M. McGrath, P. Richetti, C.M. Marques, Phys. Rev. Lett. 80 (12) (1998) 2729.
[15] W.Z. Helfrich, Naturforsh. 28c (1973) 693.
[16] F. Nallet, R. Laversanne, D. Roux, J. Phys. II France 3 (1993) 487.
[17] A. Maldonado, C. Nicot, M. Waks, R. Ober, W. Urbach, D. Langevin, J. Phys. Chem. B 108 (9) (2004) 2893.
[18] D.M. Anderson, H. Wennerström, J. Phys. Chem. 94 (1990) 8683.
[19] M.K. Doeven, J.H.A. Folgering, V. Krasnikov, E.R. Geertsma, G. van den Bogaart, B. Poolman, Biophys. J. 88 (2005) 1134.
[20] J. Israelachvili, Proc. Natl. Acad. Sci. USA 94 (1997) 8278.
[21] C. Hiergeist, R. Lipowsky, J. Phys. II France 6 (1996) 1465.